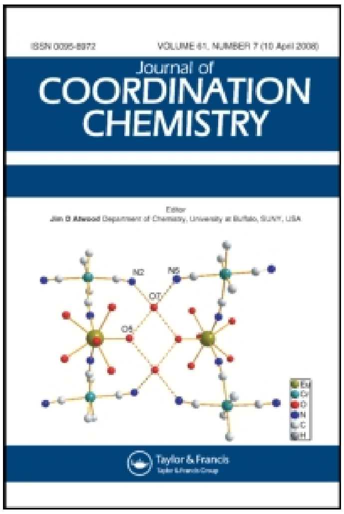

**Journal of Coordination Chemistry**
Publication details, including instructions for authors and subscription information:
http://www.informaworld.com/smpp/title~content=t713455674

# Synthesis and characterisation of $[RuCl_2(PPh_3)_2(C_{16}H_{11}NO)]$ complex

J. G. Małecki[a]
[a] Department of Inorganic and Radiation Chemistry, Institute of Chemistry, University of Silesia, 40-006 Katowice, Poland

**To cite this Article** Małecki, J. G.(2007) 'Synthesis and characterisation of $[RuCl_2(PPh_3)_2(C_{16}H_{11}NO)]$ complex', Journal of Coordination Chemistry, 60: 18, 1949 — 1958
**To link to this Article: DOI:** 10.1080/00958970601183516
**URL:** http://dx.doi.org/10.1080/00958970601183516

*Journal of Coordination Chemistry*
Vol. 60, No. 18, 15 September 2007, 1949–1958

Taylor & Francis
Taylor & Francis Group

# Synthesis and characterisation of $[RuCl_2(PPh_3)_2(C_{16}H_{11}NO)]$ complex

J. G. MAŁECKI*

Department of Inorganic and Radiation Chemistry, Institute of Chemistry,
University of Silesia, 9th Szkolna St., 40-006 Katowice, Poland

(*Received 28 April 2006; revised 11 October 2006; in final form 13 December 2006*)

The reaction of $[RuCl_2(PPh_3)_3]$ complex with 1-isoquinolyl phenyl ketone has been examined. A new ruthenium(II) complexes – $[RuCl_2(PPh_3)_2(C_{16}H_{11}NO)]$ has been obtained and characterised by IR and UV-VIS measurements. Crystal structure of the complex has been determined. The electronic spectrum of the complex has been calculated by TDDFT method.

*Keywords*: Ruthenium; N,O-donors; Phosphine; X-ray structure; TDDFT method

## 1. Introduction

The attention of the metal complexes of aldehydes and ketones as possible models for catalytic intermediates in the transfer hydrogenation of ketones by alcohols is attractive in recent years. Many ruthenium(II)-based catalysts of transfer hydrogenation are known, the species of the catalytic process remain a matter of debate. Several mechanistic proposals suggest that the key step involves activation of the coordinated substrate, making ruthenium(II) ketone and aldehyde complexes of structural interest [1]. On the other hand the transition metal complexes containing nitrogen and oxygen donors ligands have been of research interest for many years due to their steric and electronic properties [2–6].

The five-coordinate ruthenium(II) complex $[RuCl_2(PPh_3)_3]$ is well known as a very useful precursor for the preparation of wide range of ruthenium compounds, including N–donor derivatives [7–10].

The density functional theory (DFT) is a very popular computational method for the calculation of a number of molecular properties. Because of its greater computational efficiency, DFT has been applied extensively to inorganic and organometallic complexes [11–15]. The time-dependent generalization of DFT (TDDFT) offered a rigorous route to calculate the dynamic response of the charge density [16–18]. The reliability of TDDFT approach in obtaining accurate

---

*Email: gmalecki@us.edu.pl

*Journal of Coordination Chemistry*
ISSN 0095-8972 print/ISSN 1029-0389 online
DOI: 10.1080/00958970601183516

predictions of excitation energies and oscillator strengths is well documented. The method has been successfully used to calculate the electronic spectra of transition metal complexes with variety ligands [19–21]. It was found that TDDFT method gives fairly accurate results for valence excited states but incorrectly describes long-range excited states of CT character. This failure was ascribed to the self-interaction error in DFT or alternatively to incorrect asymptotic behaviour of the approximate density functional [22]. The influence of the contribution of the HF exchange in hybrid functional on the calculated energies of CT states was studied for ruthenium complexes [23].

## 2. Experimental

All reagents used to the synthesis of the complex are commercially available and were used without further purification. The $[RuCl_2(PPh_3)_3]$ complex was synthesised according to the literature method [24]. The solvent used to the reaction was argon saturated.

The complexes were prepared by adding the 1-isoquinoline phenyl ketone (0.1 g) to the solution of $[RuCl_2(PPh_3)_3]$ (0.2 g) in methanol (100 mL). The reaction mixture was stirred for 4 h. The volume of solvent was then reduced *in vacuo* to 10 mL and the precipitate was filtered off. The crystals of $[RuCl_2(PPh_3)_2(C_{16}H_{11}NO)]$ suitable for X-ray analysis was obtained by slow evaporation of the methanolic solution of the complex.

$[RuCl_2(PPh_3)_2(C_{16}H_{11}NO)]$ – Yield 65%. *Anal.* Calcd for $C_{52}H_{41}C_{l2}NOP_2Ru$: C 67.17%; H 4.44%; N 1.51%. Found: C 66.98%; H 4.29%; N 1.54%. IR (KBr): 3051 ($\nu_{CH}$); 1963($\nu_{Ph}$); 1984($\nu_{Ph}$); 1932($\nu_{Ph}$); 1579 ($\nu_{C=N}$); 1480 ($\nu_{ring}$); 1431 ($\nu_{C=C}$); 1314 ($\nu_{C=O}$); 1185 ($\delta_{CH}$); 1090 ($\delta_{CH}$); 695 ($\delta_{ring}$). UV-VIS ($CH_2Cl_2$): 645.8 (1.90) 386.0 (3.81), 265.6 (4.74), 228.4 (5.32), 215.8 (5.03).

### 2.1. *Physical measurements*

Infrared spectra were recorded on a Nicolet Magna 560 spectrophotometer in the spectral range $4000 \div 400\,cm^{-1}$ with the samples in the form of KBr pellets. Electronic spectra were measured on a spectrophotometer Lab Alliance UV-VIS 8500 in the range 800–180 nm in dichloromethane solution. Elemental analyses (C, H, N) were performed on a Perkin-Elmer CHN-2400 analyzer.

### 2.2. *Crystal structures determination and refinement*

A green plate crystal was mounted on a KM-4-CCD automatic diffractometer equipped with CCD detector, and used for data collection. X-ray intensity data were collected with graphite monochromated Mo-K$\alpha$ radiation ($0 = 0.71073$ Å) at temperature 291.0(3) K, with $\omega$ scan mode. A 12 seconds exposure time was used and all Ewald sphere was collected up to $2\theta = 50.28°$. The unit cell parameters were determined from least-squares refinement of the setting angles of 7750 strongest reflections. Details concerning crystal data and refinement are given in table 1. During the data reduction

Table 1. Crystal data and structure refinement details of [$RuCl_2(PPh_3)_2(C_{16}H_{11}NO)$].

| | |
|---|---|
| Empirical formula | $C_{52}H_{41}C_{12}NOP_2Ru$ |
| Formula weight | 929.77 |
| Temperature (K) | 291.0(3) |
| Crystal system | monoclinic |
| Space group | $P2_1/c$ |
| Unit cell dimensions (Å, °) | |
| $a$ | 9.677(3) |
| $b$ | 17.544(3) |
| $c$ | 25.791(4) |
| $\beta$ | 97.02(2) |
| Volume (Å$^3$) | 4345.5(18) |
| $Z$ | 4 |
| Calculated density (Mg m$^{-3}$) | 1.421 |
| Absorption coefficient (mm$^{-1}$) | 0.598 |
| $F(000)$ | 1904 |
| Crystal dimensions (mm$^{-3}$) | 0.598 × 0.246 × 0.057 |
| $\theta$ range for data collection (°) | 3.03 to 25.14 |
| Index ranges | $-11 \leq h \leq 11$, $-20 \leq k \leq 20$, $-0 \leq l \leq 30$ |
| Reflections collected | 15118 |
| Independent reflections | 7750 [$R_{(\text{int})} = 0.1079$] |
| Data/restraints/parameters | 7750/0/532 |
| Goodness-of-fit on $F^2$ | 0.883 |
| Final $R$ indices [$I > 2\sigma(I)$] | $R_1 = 0.0707$, $wR_2 = 0.1543$ |
| $R$ indices (all data) | $R_1 = 0.1531$, $wR_2 = 0.1934$ |
| Largest diff. peak and hole (e Å$^{-3}$) | 1.078 and −0.838 |

above decay correction coefficient was taken into account. Lorentz, polarization, and numerical absorption [25] corrections were applied. The structures were solved by direct methods and subsequently completed by the difference Fourier recycling. All the non-hydrogen atoms were refined anisotropically using full-matrix, least-squares technique on $F^2$. All the hydrogen atoms were found from difference Fourier synthesis after four cycles of anisotropic refinement, and refined as "riding" on the adjacent carbon atom with individual isotropic temperature factor equal 1.2 times the value of equivalent temperature factor of the aromatic parent carbon atom and equal 1.5 times the value of equivalent temperature factor of the methyl parent carbon atom. SHELXS97 [26], SHELXL97 [27] and SHELXTL [28] programs were used for all the calculations. Atomic scattering factors were those incorporated in the computer programs.

### 2.3. *Computational details*

Gaussian03 program [29] was used in the calculations. The geometry optimisation was carried out with the DFT method with the use of B3LYP functional [30, 31]. The electronic spectrum was calculated with the TDDFT method [32]. The DZVP basis set [33] with f functions with exponents 1.94722036 and 0.748930908 on ruthenium atom and polarization and diffuse functions to all other atoms ($6-31+g^{**}$) were used. The second calculation of electronic transitions was performed using the PCM model [34] in the dichloromethane solution as the solvent.

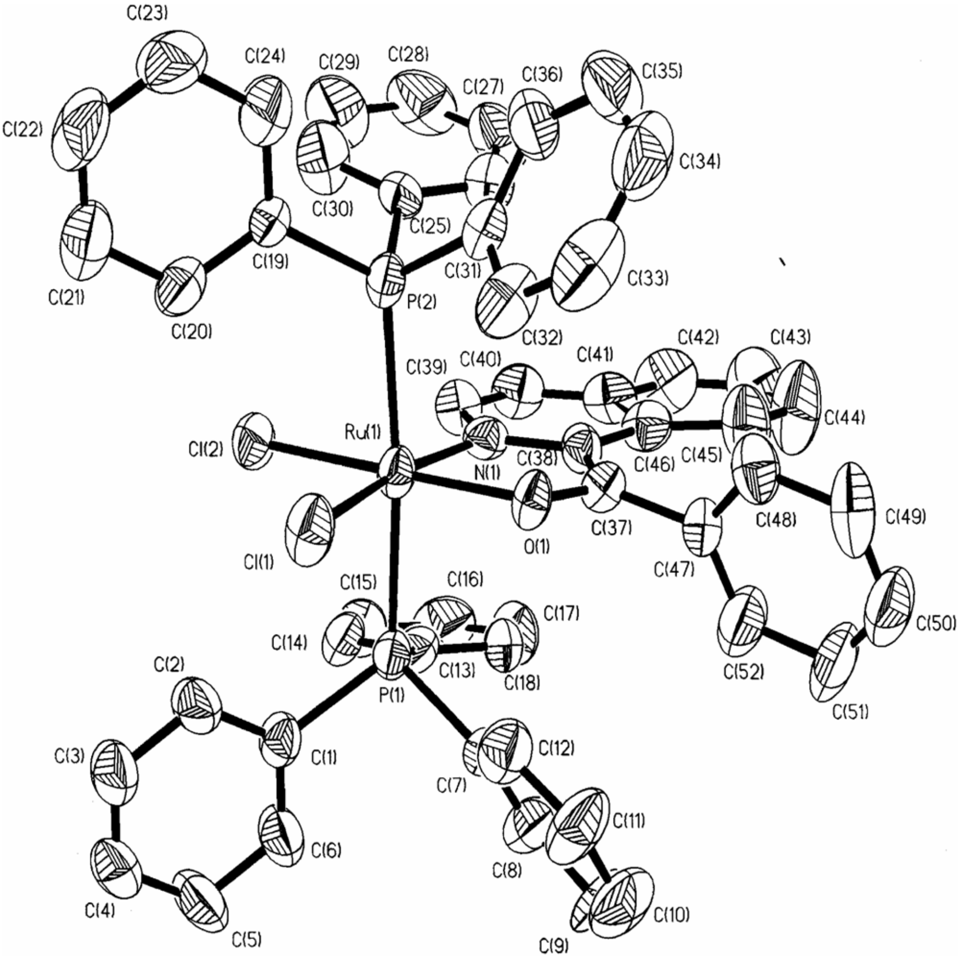

Figure 1. ORTEP drawing of $[RuCl_2(PPh_3)_2(C_{16}H_{11}NO)]$ with 50% probability thermal ellipsoids.

## 3. Results and discussion

The 1-isoquinoline phenyl ketone reacts in methanolic solutions with $[RuCl_2(PPh_3)_3]$ giving the complex $[RuCl_2(PPh_3)_2(C_{16}H_{11}NO)]$ with good yields. The elemental analysis of the complex is in good agreement with its formulation.

Infrared spectra of the complex exhibit characteristic bands due to phenyl and isoquinoline rings vibrations. The $\nu_{C=N}$ band in the complexes appeared around $1579\,cm^{-1}$. The $\nu_{C=C}$ absorption bands are visible at $1431\,cm^{-1}$.

The studied complex crystallises in the monoclinic *P2*$_1$/*c* space group. The molecular structure of the compound is shown in figure 1 (structural drawing of the complex is presented in figure 2). The selected bond lengths and angles are listed in table 2.

The ruthenium environment adopts distorted octahedral geometry with the *trans* phosphine ligands and *cis* chlorine atoms. The deviation from the ideal octahedron geometry is shown by the angles between *cis* chlorine – 95.39(8)° and the angles between

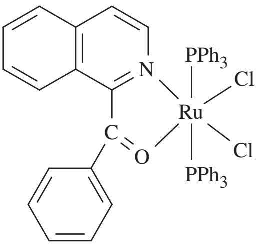

Figure 2. Structural drawing of $[RuCl_2(PPh_3)_2(C_{16}H_{11}NO)]$.

Table 2. Selected bond lengths [Å] and angles [°] for $[RuCl_2(PPh_3)_2(C_{16}H_{11}NO)]$.

| | Experimental | Calculated |
|---|---|---|
| Ru(1)–Cl(1) | 2.425(2) | 2.467 |
| Ru(1)–Cl(2) | 2.402(2) | 2.463 |
| Ru(1)–P(1) | 2.431(2) | 2.467 |
| Ru(1)–P(2) | 2.409(2) | 2.464 |
| Ru(1)–N(1) | 1.990(6) | 2.069 |
| Ru(1)–O(1) | 2.038(5) | 2.077 |
| C(37)–O(1) | 1.271(8) | 1.263 |
| N(1)–Ru(1)–O(1) | 78.0(2) | 75.94 |
| N(1)–Ru(1)–Cl(2) | 96.56(18) | 94.67 |
| O(1)–Ru(1)–Cl(2) | 174.40(15) | 170.47 |
| N(1)–Ru(1)–P(2) | 92.79(18) | 92.50 |
| O(1)–Ru(1)–P(2) | 94.33(16) | 94.01 |
| Cl(2)–Ru(1)–P(2) | 87.38(7) | 87.54 |
| N(1)–Ru(1)–Cl(1) | 167.97(17) | 168.69 |
| O(1)–Ru(1)–Cl(1) | 89.98(14) | 92.78 |
| Cl(2)–Ru(1)–Cl(1) | 95.39(8) | 96.63 |
| P(2)–Ru(1)–Cl(1) | 89.20(8) | 87.95 |
| N(1)–Ru(1)–P(1) | 88.16(18) | 92.50 |
| O(1)–Ru(1)–P(1) | 91.24(16) | 91.35 |
| Cl(2)–Ru(1)–P(1) | 87.05(7) | 87.29 |
| P(2)–Ru(1)–P(1) | 174.42(7) | 172.83 |
| Cl(1)–Ru(1)–P(1) | 91.02(8) | 87.70 |

Table 3. Hydrogen bonds for $[RuCl_2(PPh_3)_2(C_{16}H_{11}NO)]$ (Å and °).

| D–H···A | d(D–H) | d(H···A) | d(D···A) | ∠(DHA) |
|---|---|---|---|---|
| C(2)–H(2)···Cl(1) | 0.93 | 2.72 | 3.431(10) | 133.5 |
| C(20)–H(20)···Cl(1) | 0.93 | 2.79 | 3.341(8) | 119.1 |
| C(20)–H(20)···Cl(2) | 0.93 | 2.69 | 3.403(9) | 134.6 |
| C(39)–H(39)···Cl(2) | 0.93 | 2.71 | 3.322(9) | 124.4 |
| C(40)–H(40)···Cl(1)#1 | 0.93 | 2.57 | 3.493(9) | 172.1 |

*trans* phosphine molecules – 174.42(7)°. All Ru-ligand distances, such as Ru–Cl 2.425(2) Å, 2.402(2) Å, Ru–P 2.431(2) Å, 2.409(2)Å and Ru–N 1.990(6) Å and Ru–O 2.038(5) Å, are normal and comparable with distances in other ruthenium complexes containing the heterocyclic ligands [35–38].

The conformation of molecule is stabilised by four C–H···Cl weak intramolecular hydrogen bonds [23–25] (D···A distance varies from 3.431(10) to 3.322(9) Å and

D–H ··· A angle varies from 134.6 to 119.1°), one C(18)–H(18) ··· N(1) and one intermolecular hydrogen bond linking C(40)–H(40) ··· Cl(1)#1 (#1 $x+1, y, z$) (D ··· A distance 3.493(9) Å, D–H ··· A angle 172.1°) (see table 3).

### 3.1. *Geometry and electronic structure*

The optimised geometry parameters for the studied complex are given in table 2. The calculated bond lengths and angles for the $[RuCl_2(PPh_3)_2(C_{16}H_{11}NO)]$ agree with the experiment, the largest difference are found for the ruthenium–chlorine and Ru–P bonds (~0.06 Å).

The formal charge of ruthenium is +2 in this complex. The calculated charge on the ruthenium atom, obtained from natural population analysis, is close 0.494. The population of the $d_{xy}$, $d_{xz}$, $d_{yz}$, $d_{x^2-y^2}$ and $d_{z^2}$ orbitals of the central atom is following 1.640, 1.893, 0.690, 1.243 and 1.732, respectively. This is a result of charge donation from chlorine ligands (charge –0.576) and phosphine molecules (total charge on $PPh_3$ 0.318; 0.317) to ruthenium atom. The charge on the 1-isoquinoline phenyl ketone, obtained from NBO analysis, is close to 0.023. The HOMO–LUMO gap is 1,79 eV.

In figure 3 the molecular orbital diagram is presented with several HOMO (figure 3a) and LUMO (figure 3b) contours of molecular orbitals. The $d_{yz}$, $d_{xz}$, $d_{xy}$ ruthenium orbitals are visible in the Homo, Homo-1 and Homo-2 molecular orbitals with an antibonding contribution from $\pi$ chlorine ligands. The phosphorus lone pair takes part in Homo-2 molecular orbital. The Homo-3 molecular orbital is composed from P phosphine lone pairs with antibonding contribution of $\pi$ chlorine orbitals. The Homo-4 MO is composed of $\pi$ chlorine orbitals. The $\pi$ carbonyl oxygen orbitals are visible in the Homo-9 molecular orbital with the contribution of $\pi$ benzene orbitals. The LUMO molecular orbital is composed of ruthenium $d_{x^2-y^2}$ with antibonding contribution of nitrogen 1-isoquinoline phenyl ketone and the carbon orbitals. The $d_{z^2}$ Ru orbital composed the Lumo + 3 MO with antibonding contribution $\sigma$(lone pairs) of phosphorus orbitals. The ketone oxygen orbitals are visible in the Lumo + 7 molecular orbital with shares of $d_{x^2-y^2}$ ruthenium orbital. The Lumo + 1 and Lumo + 2 orbitals are resulted from 1-isoquinoline phenyl ketone orbitals. The $\pi$ oxygen and nitrogen orbitals play role in the Lumo + 1 MO.

### 3.2. *Electronic spectrum*

The investigated complex is of large size, and the number of basis functions is equal to 960. Hundred electron transitions calculated by the TDDFT method do not comprise all the experimental absorption bands. The UV-Vis spectrum was calculated to 255 nm, so the shortest wavelength experimental bands cannot be assigned to the calculated transitions. However, considering that the solution spectra of $PPh_3$ and 1-isoquinoline phenyl ketone exhibit intense absorption bands in 260–200 nm region, some additional intraligand and interligand transitions are expected to be found at higher energies in the calculations.

The calculated and experimental spectra of $[RuCl_2(PPh_3)_2(C_{16}H_{11}NO)]$ are depicted on figure 4. In the figure 4(b) and (c) are presented the transitions obtained from the calculations with and without PCM model respectively. The effect of the solvent on the calculated electronic spectrum of the investigated complex is mainly visible in the

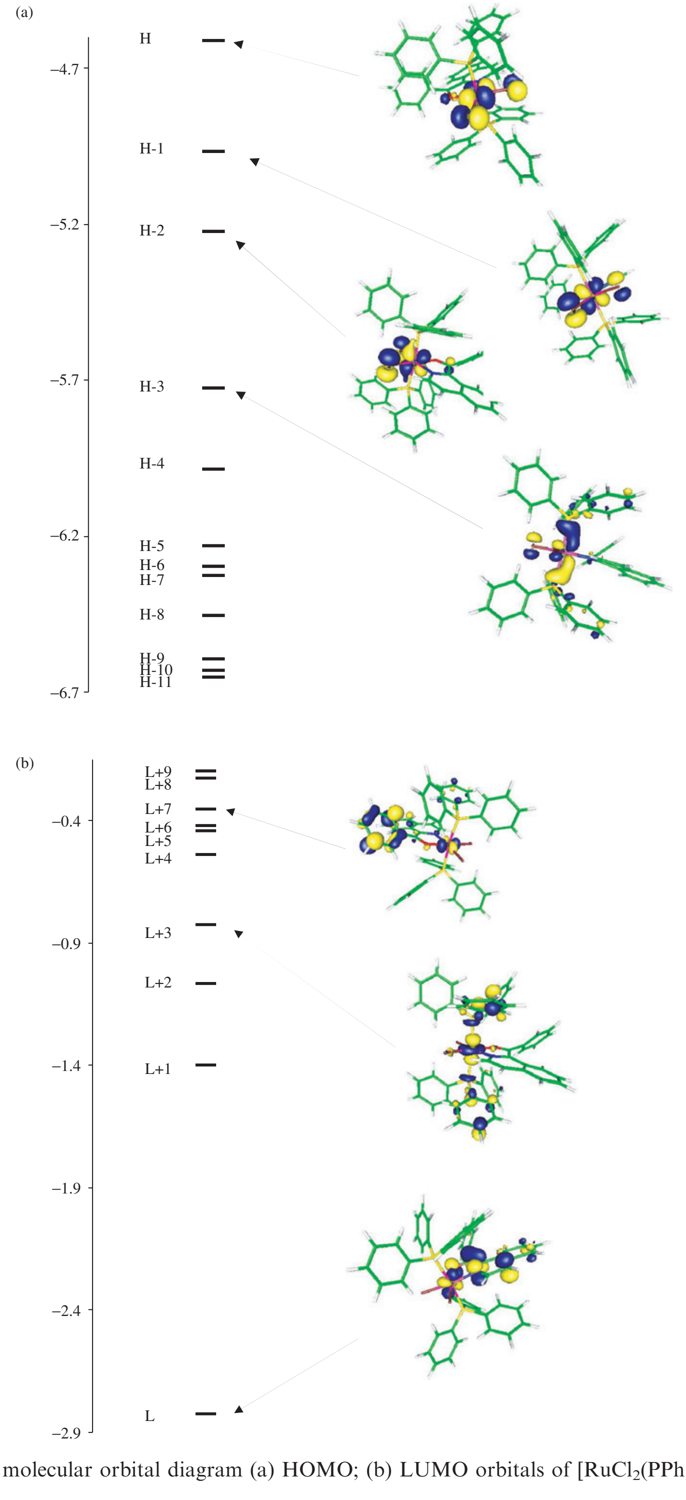

Figure 3. The molecular orbital diagram (a) HOMO; (b) LUMO orbitals of [$RuCl_2(PPh_3)_2(C_{16}H_{11}NO)$].

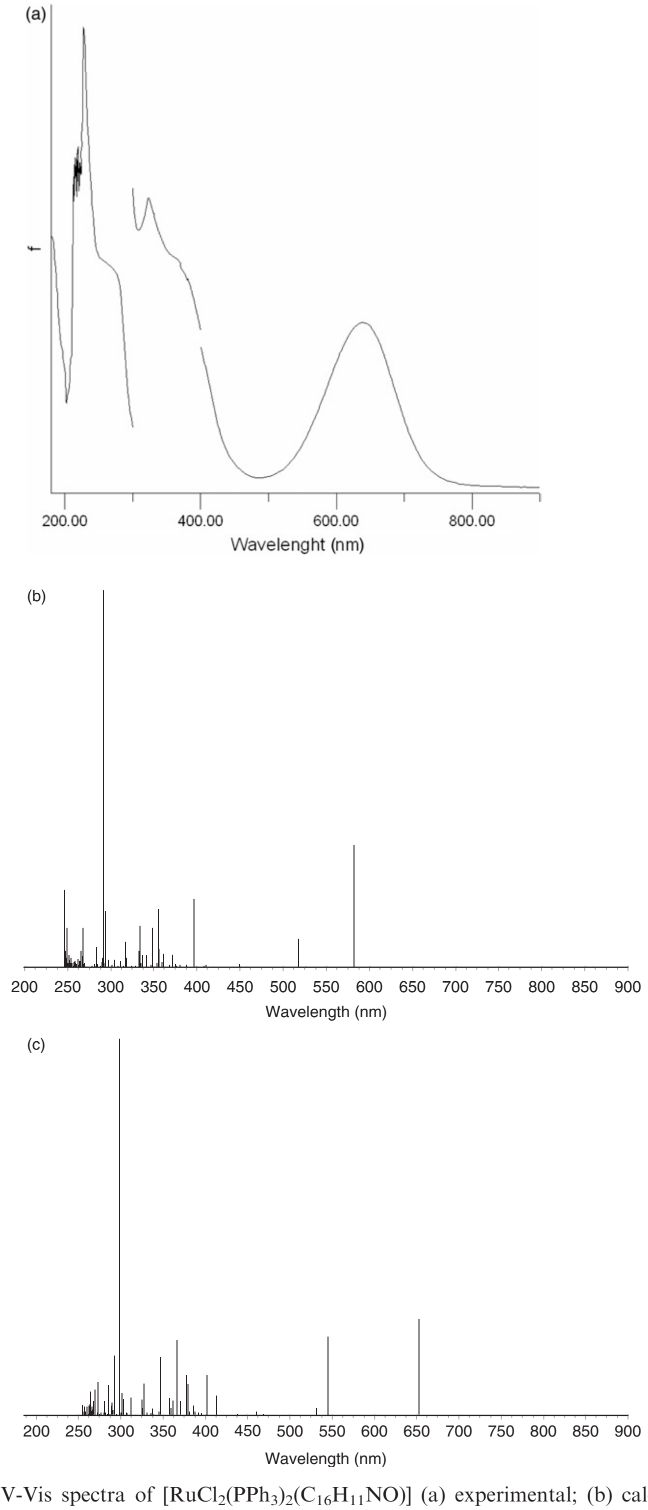

Figure 4. The UV-Vis spectra of [$RuCl_2(PPh_3)_2(C_{16}H_{11}NO)$] (a) experimental; (b) calculated with PCM model; (c) calculated without solvent.

intense of the calculated electronic transitions. The average difference between energy of the corresponding transitions is close to 0.19 eV (6.5 nm).

The longest wavelength experimental broad band with maximum at 642.8 nm is assigned to the transitions from HOMO-2 and HOMO-3 to LUMO orbitals. As the LUMO orbital has a substantial admixture of $\pi^*$ orbitals of the isoquinoline ring, these transitions are classified as $d \rightarrow d/\pi^*_{QPhCO}$. It explains a relatively high value of the oscillator strength of the calculated excitation at 642.8 nm.

The experimental absorption band at 370.0 nm is attributed to the transitions calculated between 413.2 and 366.8 nm. These are excitations from central metal $d$ orbitals to the $\pi^*$ orbitals of the 1-isoquinoline phenyl ketone ligand.

The absorption band at 323.4 nm is ascribed to the metal–ligand charge transfer transitions ($d \rightarrow \pi^*_{QPhCO}$ and $d \rightarrow \pi^*_{Ph}$). The last calculated transitions attributed to experimental one at 227.8 nm occur mainly from the $d$ ruthenium orbitals with admixture of $\pi$ chloride and phosphorus lone pair orbitals to $\pi^*_{Ph}(PPh_3)$. The ligand-ligand charge transfer resulted from $\pi_{Ph} \rightarrow \pi^*_{QPhCO}$ are observed in this band.

The experimental band at 215.8 nm could not be assigned on the basis of the calculated transitions; it can be assumed that the band results from transitions in the $PPh_3$ ligands and the $\pi \rightarrow \pi^*$ excitations in the 1-isoquinoline phenyl ketone ligand.

## Supplementary material

More details of the crystal structure determinations have been deposited with the Cambridge Crystallographic Data Centre with the deposition number: CCDC 288860.

## Acknowledgements

The Gaussian03 calculations were carried out in the Wrocław Centre for Networking and Supercomputing, WCSS, Wrocław, Poland under calculational grant No 51/96.

## References

[1] M. Yamakawa, H. Ito, R. Noyari. *J. Am. Chem. Soc.*, **122**, 1466 (2000).

[2] S. Chang, L. Jones, C.M. Henling, R.H. Grubbs. *Organometallics*, **17**, 3460 (1998).

[3] B. De Clereq, F. Verpoort. *Macromolecules*, **35**, 8943 (2002).

[4] B. De Clereq, F. Verpoort. *Adv. Synth. Catal.*, **34**, 639 (2002).

[5] T. Opstal, F. Verpoort. *Angew Chem. Int. Ed.*, **42**, 2876 (2003).

[6] B. De Clereq, F. Lefebvre, F. Verpoort. *Appl. Catal. A*, **247**, 345 (2003).

[7] F. Porta, S. Tollari, C. Bianchi, S. Recchia. *Inorg. Chim. Acta*, **249**, 79 (1996).

[8] S.L. Queiroz, A.A. Batista, G. Olivia, M.T. do, P. Gambardella, R.H.A. Santos, K.S. MacFarlane, S.J. Rettig, B.R. James. *Inorg. Chimica Acta*, **267**, 209 (1998).

[9] I.R. Butler, U. Griesbach, P. Zanello, M. Fontani, D. Hibbs, B.M. Hursthouse. *J. Organomet. Chem.*, **565**, 243 (1998).

[10] J.G. Małecki, J.O. Dzięgielewski, R. Kruszynski, T.J. Bartczak. *Inorg. Chem. Commun.*, **6**, 721 (2003).

[11] P.C. Hohenberg, W. Kohn, L.J. Sham. *Adv. Quantum Chem.*, **21**, 7 (1990).

[12] W. Kohn, A.D. Becke, R.G. Parr. *J. Phys. Chem.*, **100**, 12974 (1996).

[13] R.G. Parr, W. Yang. *Ann. Rev. Phys. Chem.*, **46**, 701 (1995).

[14] E.J. Baerends, O.V. Gritsenko. *J. Phys. Chem.*, **A 101**, 5383 (1997).
[15] T. Ziegler. *Chem. Rev.*, **91**, 651 (1991).
[16] M.E. Casida, (D.P. Chong. *Recent Advances in Density Functional Methods*, Vol. 1, World Scientific, Singapore (1995).
[17] M.E. Casida, (J.M. Seminario. Recent Developments, & Applications of Modern Density Functional Theory. *Theoretical and Computational Chemistry*, Vol. 4, p. 391, Elsevier, Amsterdam (1996).
[18] M.E. Casida, C. Jamorski, K.C. Casida, D.R. Salahub. *J. Chem. Phys.*, **108**, 4439 (1998).
[19] C. Adamo, V. Barone. *Theor. Chem. Acta*, **105**, 169 (2000).
[20] S.J.A. van Gisbergen, J.A. Groeneveld, A. Rosa, J.G. Snijders, E.J. Baerends. *J. Phys. Chem. A*, **103**, 6835 (1999).
[21] A. Rosa, E.J. Baerends, S.J.A. van Gisbergen, E. van Lenthe, J.A. Groeneveld, J.G. Snijders. *J. Am. Chem. Soc.*, **121**, 10356 (1999).
[22] A. Dreuw, M. Head-Gordon, J. Am. Chem. Soc., 126 (2004) 4007; A. Dreuw, J.L. Weisman, M. Head-Gordon, *J. Chem. Phys.*, 119 (2003) 2943; O. Gritsenko, E. J. Baerends, *J. Chem. Phys.*, **121**, 655 (2004).
[23] S. Záliš, N. Ben Amor, C. Daniel. *Inor. Chem.*, **43**, 7978 (2004).
[24] T.A. Stephenson, G. Wilkonson. *J. Inorg. Nucl. Chem.*, **28**, 945 (1966).
[25] X-RED. Version 1.18. STOE & Cie GmbH, Darmstadt, Germany (1999).
[26] G.M. Sheldrick. *Acta Cryst.*, **A46**, 467 (1990).
[27] G.M. Sheldrick. *SHELXL97. Program for the Solution and Refinement of Crystal Structures*, University of Göttingen, Germany (1997).
[28] G.M. Sheldrick. *SHELXTL: release 4.1 for Siemens Crystallographic Research Systems* (1990).
[29] R. Mukherjee. *Coord. Chem. Rev.*, **203**, 151 (2000).
[30] Gaussian 03, Revision B.03, M.J. Frisch, G.W. Trucks, H.B. Schlegel, G.E. Scuseria, M.A. Robb, J.R. Cheeseman, J.A. Montgomery Jr, T. Vreven, K.N. Kudin, J.C. Burant, J.M. Millam, S.S. Iyengar, J. Tomasi, V. Barone, B. Mennucci, M. Cossi, G. Scalmani, N. Rega, G.A. Petersson, H. Nakatsuji, M. Hada, M. Ehara, K. Toyota, R. Fukuda, J. Hasegawa, M. Ishida, T. Nakajima, Y. Honda, O. Kitao, H. Nakai, M. Klene, X. Li, J.E. Knox, H.P. Hratchian, J.B. Cross, C. Adamo, J. Jaramillo, R. Gomperts, R.E. Stratmann, O. Yazyev, A.J. Austin, R. Cammi, C. Pomelli, J.W. Ochterski, P.Y. Ayala, K. Morokuma, G.A. Voth, P. Salvador, J.J. Dannenberg, V.G. Zakrzewski, S. Dapprich, A.D. Daniels, M.C. Strain, O. Farkas, D.K. Malick, A.D. Rabuck, K. Raghavachari, J.B. Foresman, J.V. Ortiz, Q. Cui, A.G. Baboul, S. Clifford, J. Cioslowski, B.B. Stefanov, G. Liu, A. Liashenko, P. Piskorz, I. Komaromi, R.L. Martin, D.J. Fox, T. Keith, M.A. Al-Laham, C.Y. Peng, A. Nanayakkara, M. Challacombe, P.M.W. Gill, B. Johnson, W. Chen, M.W. Wong, C. Gonzalez J.A. Pople, Gaussian, Inc., Pittsburgh PA, 2003.
[31] A.D. Becke. *J. Chem. Phys.*, **98**, 5648 (1993).
[32] C. Lee, W. Yang, R.G. Parr. *Phys. Rev. B*, **37**, 785 (1988).
[33] N. Godbout, D.R. Salahub, J. Andzelm, E. Wimmer. *Can. J. Chem.*, **70**, 560 (1992).
[34] B. Mennucci, J. Tomasi. *J. Chem. Phys.*, **106**, 5151 (1997).
[35] R. Mukherjee. *Coord. Chem. Rev.*, **203**, 151 (2000).
[36] T. Hirano, M. Kuroda, N. Takeda, M. Hayashi, M. Mukaida, T. Oi, H. Nagao. *J. Chem. Soc. Dalton Trans.*, 2158 (2002).
[37] A.C.G. Hotze, M. Bacac, A.H. Velders, B.A.J. Jansen, H. Kooijman, A.L. Spek, J.G. Haasnoot, J. Reedijk. *J. Med. Chem.*, **46**, 1743 (2003).
[38] Ka-Lai Yip, Wing-Yiu Yu, Pui-Ming Chan, Nian-Yong Zhu, Chi-Ming Che. *Dalton Trans.*, 3556 (2003).